

See discussions, stats, and author profiles for this publication at: <https://www.researchgate.net/publication/228571758>

# Taxicab geometry: Some problems and solutions for square grid-based fire spread simulation

Article in *Forest Ecology and Management* · November 2006

DOI: 10.1016/j.foreco.2006.08.134

---

CITATIONS

13

---

READS

2,648

1 author:



David Caballero

MeteoGRID

57 PUBLICATIONS 663 CITATIONS

SEE PROFILE

# Taxicab Geometry: some problems and solutions for square grid-based fire spread simulation

David Caballero

*Tecnoma S.A., Isla del Hierro 7, S.S. de los Reyes, 28700 Madrid, Spain*  
*davidcaballero@tecnoma.es*

---

**Abstract:** Many of the existing fire spread simulation applications make use of square-cell grid based maps, a solution that is not free of problems due to the discrete interpretation of reality and the segmentation of space into geometric shapes. These particularities entail systematic errors when programming cellular automata for forest fire simulation, particularly in the computation of distances, hence delivering erroneous simulations of fire front size and position. Inspired in the concept of taxicab geometry, coined by Minkowsky in the 19<sup>th</sup> century, a new one, that has been labelled here as 'Extended Taxicab Geometry' and which underlies in most of the grid-based fire spread automata, is described in this paper. Algorithmic improvements for the computer code to avoid unwanted effects in the simulations are also presented. A second common problem, appearing when the elliptical shape associated to spread propagation is too narrow, is described, and an algorithmic solution is proposed for its implementation in a computer program.

**Keywords:** spread simulation, square grid, geometry, taxicab

## 1. Introduction

Today is common to see forest fire spread simulation applications running in several of the operational centres across Europe. Once just a subject of research, these computer tools become popular mostly among new generations of fire managers as a complement for decision making. However it is also frequent to see that simulation tools are not used and interpreted adequately to obtain the desired results. Inaccurate inputs, incomplete or inexperienced operation and straight-forward interpretation of results commonly lead to unrealistic assessments, hence entailing a progressive loss of confidence of fire managers on such computer tools.

To this, we have to add the fact that the existing computer applications for forest fire simulation are themselves not exempt of inaccuracy. Being a complex phenomenon, forest fires normally entail intricate mathematical and physical formulation, and in the most successful cases a complex computer code. Due to this, the simpler or more practical approaches to the problem, such as the semi-empirical model of Frandsen-Rothermel, have had a tremendous success among computer programmers for the development of fire spread simulation applications.

Besides to this, it is important to consider the inherent complexity of geographical information as well, and the associated information systems (GIS) developed to make the world easier to a vast number of users, particularly fire modellers. Digital maps are presented as a particular type of information entities, based in paradigms and spatial geometries, which allow measuring distances and locating items in the world space. But as

we accept the telephone sound quality (which normally is very poor) to be good enough to be considered as 'real', we usually accept digital maps and all their associated limitations to be good enough to represent geographical reality. However, we must be careful and always remember that this offered solution is just that, a representation of reality, and that has its own particularities that could show off anytime and create difficulties.

In particular, many of the existing forest fire spread simulation applications makes use of square-cell grid maps (usually known as 'raster maps'), a geometric solution widely used in the representation of reality in environmental management issues. But this solution is not free of problems due to the discrete interpretation of reality (information granularity) and the rigid segmentation of space into geometric shapes (square cells), which ends-up in a quantised solution space (the grid). Without taking care of them, the associated particularities of this geometry entail systematic errors when, for example, programming cellular automates for fire simulation, and more particularly in the computation of distances, hence delivering erroneous simulations of fire front size and position.

The purpose of this paper is to highlight and describe some of such particularities and also address some associated problems found in the design and programming of a specific fire spread simulation application.

## **2. Mechanism of a fire spread cellular automaton**

Several of the computer-based forest fire spread applications (i.e. FIRESTATION, FMIS, CARDIN, FSE) base their operation in the same general idea of a cellular automata that calculates the time spent by fire travelling from one cell to the surrounding eight ones. Given that the distance between cells is easily estimated by considering the one separating each cell's centroid, the time spent by the fire to travel from one cell to a neighbouring one is obtained by dividing such distance by the propagation speed projected in such direction.

The Fire Spread Engine (FSE) presented here, which is based in an adapted version of the one found in CARDIN simulation system (Martínez-Millán 1991; Caballero, 1994), should serve as an example of what is the subject of this paper. Although, as said, each model has its own particularities, the purpose of a general explanation of commonalities found in cellular automata can be well covered with this example. The FSE application is the result of a permanent evolution and improvement of the original code of CARDIN. This has been achieved along several research projects over the last years, such as FOMFIS (Caballero, 1999), E-FIS (Caballero, 2001); FORFAIT, AUTOHAZARD and WARM, all of them funded by the European Commission.

As mentioned, the engine bases its operation in a cellular automaton that calculates the time spent by fire travelling from one cell to the eight surrounding ones. The process, essentially, is simple: the basic spread law is calculated using the values encountered in the analysing cell (A) relative to slope, aspect, fuel model, and wind direction and intensity. For each spread direction, corresponding to each of the eight neighbouring cells, a projection of the basic spread law is obtained, giving the value of propagation for such direction. As distance among cell is easily estimated by considering the centres position of

each cell, the time spent by the fire to travel from one centre to the other is obtained by dividing the distance by the projected speed.

Each of the surrounding cells of a given analysing cell  $A$  has a unique direction of analysis, identified by a number from 1 to 8, clockwise from north position corresponding to value 1, and an angle multiple of  $45^\circ$  (0, 45, 90, etc.) . Let the analysing cell will be  $A$ , the analysed cell  $B$  and the reference cell  $R$ . The reference cell corresponds to the latest position where significant changes in some of the spread law factors (slope, aspect, wind or fuel) were found (see further explanations in point 5 of this paper). For the first analysing cell (position of the fire outbreak) the reference cell is itself and the same applies for the first eight surrounding cells being analysed. With this, a matrix holding the information of each cell, looking much like this, governs all the process:

8	1	2
7	A	3
6	5	4

PTR	X	Y	t	$I_R$

In this matrix,  $PTR$  (pointer) is an index, ranging from 1 to the total number of analysed cells, which sorts all cells according the value of the fire access time  $t$  in ascending order;  $X$  and  $Y$  are the correspondent column and row of the cell in the grid;  $t$  is the calculated time that fire takes to reach such point and  $I_R$  is the position in the matrix (index) of the reference cell. This matrix is being continuously updated as the simulation progresses, as each new cell resulting from the analysis is inserted and sorted according the fire access time  $t$ . When a fire starts a new matrix is generated and a first new cell is inserted, for example:

	PTR	X	Y	t	$I_R$
>	1	100	100	0	1

The position is the current position of the cell where fire starts; the access time  $t$  is the moment in which the fire starts and the reference position, for this case, is the cell itself, as there is no other cell to which refer the analysis. Once the matrix is feed first time, then the process runs iteratively. The process advances to the next pointer position in the matrix and reads the values required for spread law calculation.

The basic spread law procedure returns the maximum spread rate and the direction of maximum spread. These values are used to obtain the spread rate in each of the eight surrounding directions by projecting the obtained basic spread law. For each of the eight directions the procedure obtains the position  $X_B$ ,  $Y_B$ , of the neighbouring analysed cells. The distance and the direction angle between each  $A - B$  pairs is directly obtained by:

DIR	$X_B$	$Y_B$	Angle	Distance
1	$X_A$	$Y_A+L$	$0^\circ$	$L$
2	$X_A+L$	$Y_A+L$	$45^\circ$	$L\sqrt{2}$
3	$X_A+L$	$Y_A$	$90^\circ$	$L$
4	$X_A+L$	$Y_A-L$	$135^\circ$	$L\sqrt{2}$
5	$X_A$	$Y_A-L$	$180^\circ$	$L$
6	$X_A-L$	$Y_A-L$	$225^\circ$	$L\sqrt{2}$
7	$X_A-L$	$Y_A$	$270^\circ$	$L$
8	$X_A-L$	$Y_A+L$	$315^\circ$	$L\sqrt{2}$

In the table,  $X_A$ ,  $Y_A$  is the position of the analysing cell and  $L$  the cell resolution. In the process, eight new entries are inserted and sorted in the matrix, progressing in the analysis by moving the pointer to the next position. This is continuously repeated until the simulation time (specified by modeller) is reached, or if there are no more cells to analyse.

	PTR	X	Y	t	$I_R$
R	1	100	100	0	1
>	2	100	101	7	1
	3	99	101	8	1
	4	101	101	8	1
	5	99	100	10	1
	6	101	100	10	1
	7	99	99	12	1
	8	101	99	12	1
	9	100	99	15	1

But at this point it was observed that the calculation of the distance existing between two separate (not neighbouring) cells, for example  $R$  and  $B$  (Fig. 1), and as the result of successive addition of discrete distances of  $L$  and  $L\sqrt{2}$ , entailed an error in excess when compared with the correspondent Euclidean distance  $RB$ .

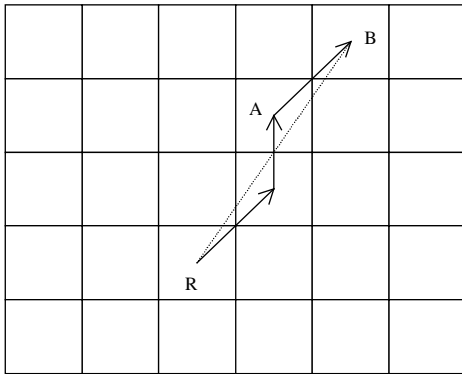


**Fig. 1.** The Euclidean distance between two points ( $RB$ ) is increased when following a discretised path ( $RAB$ ). Consequently the calculated invested time to pass from  $R$  to  $B$  is increased proportionally.

This error became more evident in the directions of analysis between those that were multiple of 45 degrees. For these, the Euclidean distances and the automata distances resulted to be the same. Given the importance of this effect in the final simulation, which was rendering kite-like shapes instead of elliptical forms and providing defective predictions of areas and distances, a deeper analysis of the underlying geometry was needed to characterise and solve the problem.

### 3. Taxicab geometry

Taxicab geometry (hereinafter also addressed as “taxigeometry”), considered by Hermann Minkowski in the 19<sup>th</sup> century, is a form of geometry in which the usual metric of Euclidean geometry is replaced by a new metric in which the distance between two points is the sum of the (absolute) differences of their coordinates (Krause, 1987). More formally, we can define the Manhattan distance, also known as the L1-distance, between two points in an Euclidean space with fixed Cartesian co-ordinate system is defined as the sum of the lengths of the projections of the line segment between the points onto the coordinate axes (Fig. 2). For example, in the plane, the Manhattan distance  $T$  between the point  $A$  with coordinates  $(X_A, Y_A)$  and the point  $B$  at  $(X_B, Y_B)$  is:

$$T = |X_B - X_A| + |Y_B - Y_A| \quad (1)$$

while for the Euclidean distance  $E$  for the same points is calculated by:

$$E^2 = (X_B - X_A)^2 + (Y_B - Y_A)^2 \quad (2)$$

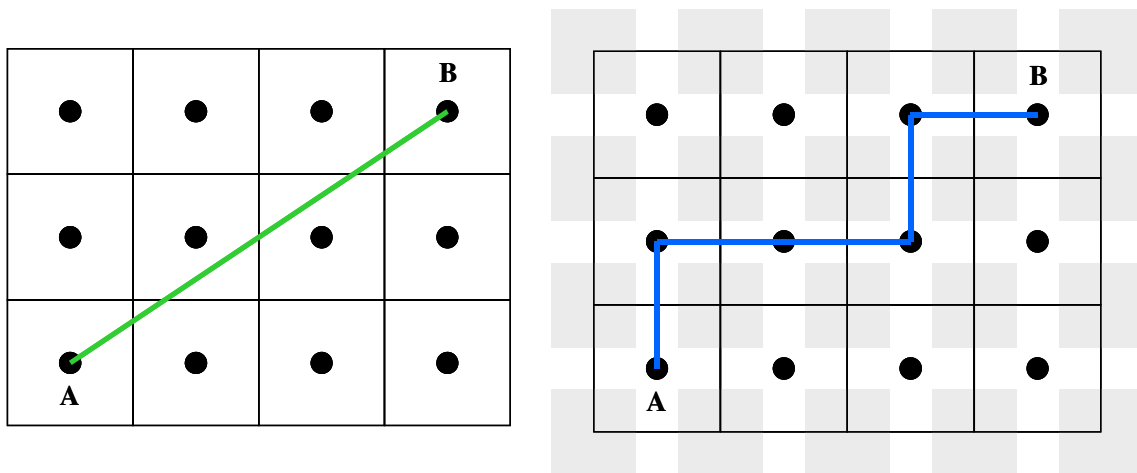


**Fig. 2.** In the Euclidean space (left) the distance between two points A and B is obtained without restrictions. In the taxicab space (right) the same distance is obtained by accumulating vertical and horizontal segments, like a taxi cab driving through the streets of a city compound of equal, adjacent square blocks. The total run is the sum of all segments, which coincides with the sum of the difference of vertical and horizontal co-ordinates of points A and B. It is easy and intuitive to see that the taxicab distance is equal or great than the Euclidean one.

#### 4. Extended Taxicab Geometry

For the definition of the geometry underlying in the calculation of fire spread using cellular automata, characterised by a central cell and eight neighbouring ones, an extended definition of the taxicab geometry is required, in which diagonal distance to the cells placed in the opposite corners is also considered. Inspired in the idea of taxicab, the extended taxicab distance can be understood as the path of a taxi cab moving from a point A to other B in a city compound of adjacent square buildings but with two internal corridors that allow the cars to pass freely from one corner to the other in diagonal (Fig. 3).

The Extended Taxicab Geometry is consistent with the procedure of the automata algorithms presented above and the associated extended taxicab distance between two generic points A and B in the plane can be easily deduced (Fig. 4)

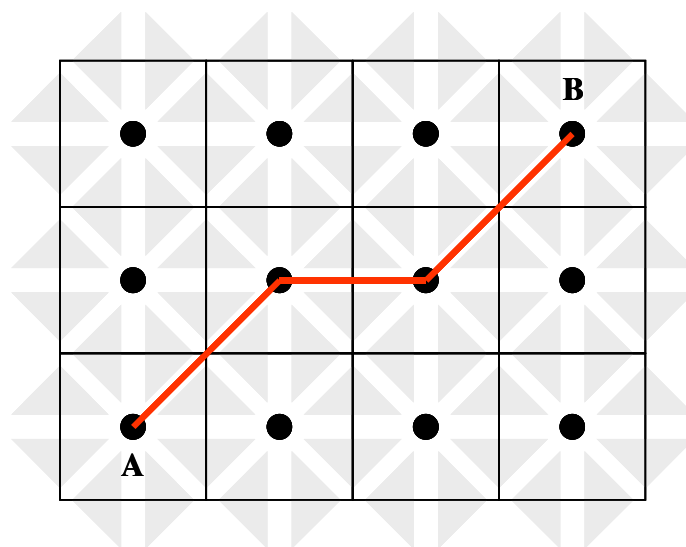


**Fig. 3.** Extended taxicab geometry, is that of a city compound of square adjacent blocks with two internal corridors forming an 'X' and allowing the free, direct transit between two opposite corners of the same building.

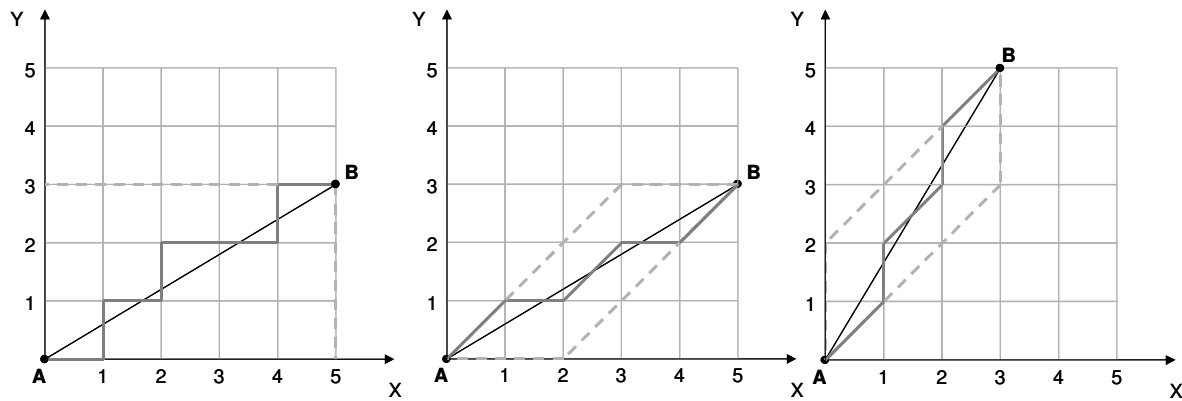


Fig. 4. Differences in the calculation of the taxicab distance (left) and the extended taxicab distance (centre and right)

Each pair of points  $A$  and  $B$  in the plane define a parallelogram by the projection of seldom lines forming 45 degrees with the co-ordinate axis. Within the extension of this resulting parallelogram, it is easy to deduce that the extended taxicab distance is the same, whatever alternative path is taken, always respecting the extended taxicab rule of connecting two opposite corners by a diagonal (a minimum distance criterion).

In light of this, the extended taxicab distance  $T_e$  can be defined as the sum of number of straight segments  $U$  and the number of diagonals  $D$  multiplied by the square root of two, where  $U$  is the absolute difference between the biggest co-ordinate difference of points  $A$  and  $B$  and the smallest one, and  $D$  the smallest co-ordinate difference of  $A$  and  $B$ :

$$\begin{aligned} T_e &= U + D * \text{SQRT}(2) \\ U &= \text{Max} ( |X_B - X_A|, |Y_B - Y_A| ) - \text{Min} ( |X_B - X_A|, |Y_B - Y_A| ) \\ D &= \text{Min} ( |X_B - X_A|, |Y_B - Y_A| ) \end{aligned} \quad (3)$$

With the expressions (1) and (3) it is easy to compute the values of the taxicab distance and the extended taxicab distance for all points of a region. Moreover, making use of expression (2) it is also possible to calculate the differences  $T-E$  and  $T_e-E$  for all points, thus providing a synthetic view of the ‘distortion map’ of the distances due to taxigeometry in both cases when compared to the Euclidean space (Fig. 5)

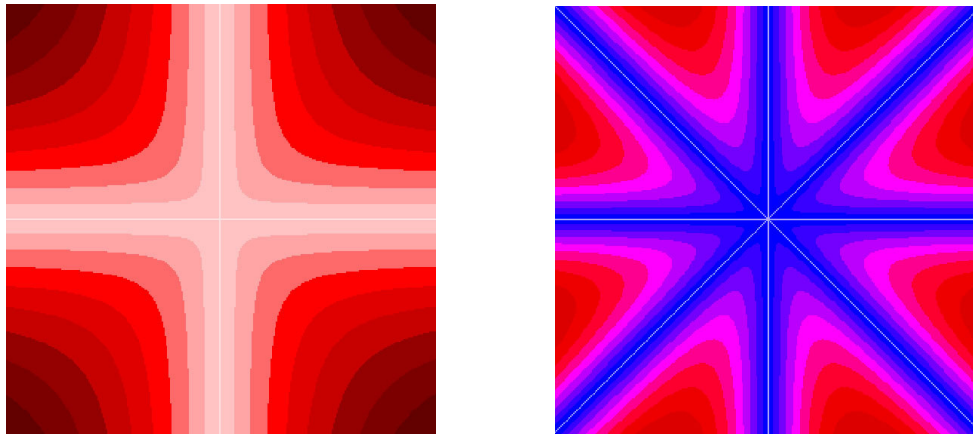
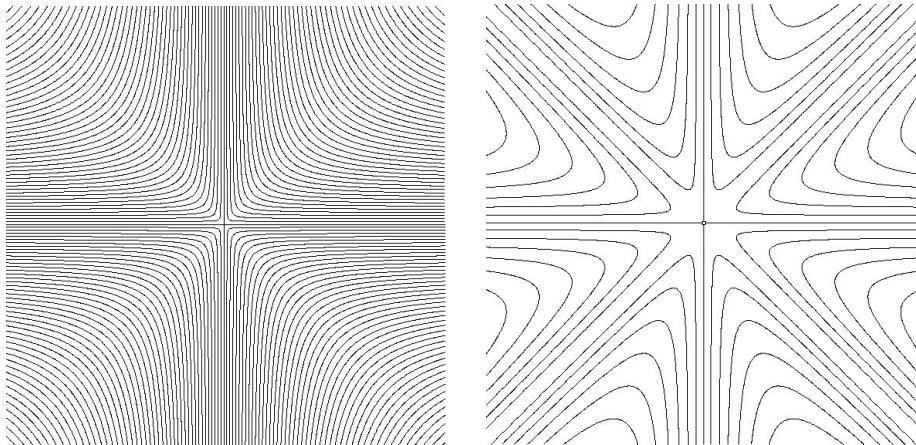


Fig. 5. Distortion maps corresponding to the taxicab geometry (left) and the extended taxicab geometry (right). In both cases the axes along which Euclidean and taxicab distances coincide (non-distortion axes) are clearly identified. For the rest of the points, a noticeable difference is observed between the segments of 90° (left) and 45° (right).

Looking more in detail to these distortion maps (see also Fig. 6), is interesting to observe that along four axes in the taxicab and eight in the extended taxicab geometry the Euclidean distances coincide exactly with the taxicab distances. Near the centre the difference is less noticeable, as well as in the vicinity of the non-distortion axes, but the difference rapidly increases in points located far away of these particularities.

The most evident and perhaps important observation is that the maximum difference occurs in the angles between the non-distortion axes (multiples of  $90^\circ$  in the taxicab and multiples of  $45^\circ$  in the extended taxicab), thus summing the effect in the points located away from the centre. The distortion map is better understood when looking at the 3D representation (Fig. 7).



**Fig. 6.** Distortion maps corresponding to the taxicab geometry (left) and the extended taxicab geometry (right) represented by isolines at the same interval in both cases for comparison. Observe how quickly the distortion increases in the taxicab space when compared with the extended taxicab space. The distortion increases dramatically outside the centre and the non-distortion axes in both cases.

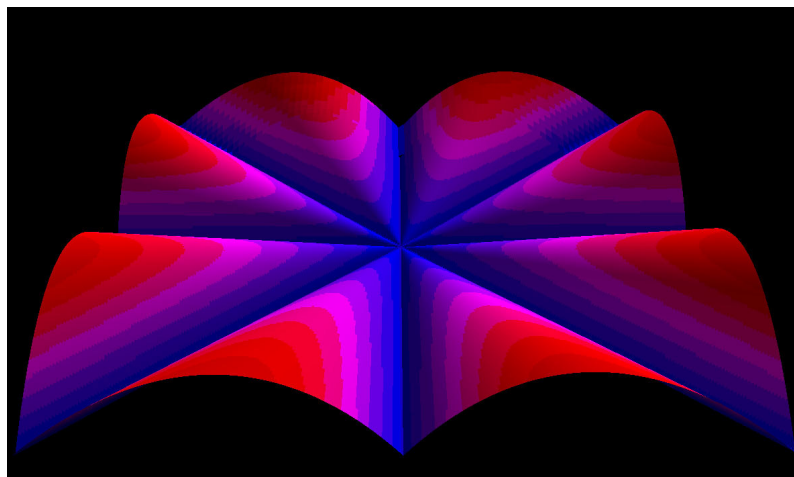


**Fig. 7.** Distortion map of the extended taxicab space represented in 3D. This three-dimensional projection helps to understand and remember the importance of the underlying particularities of this geometry in the computation of distances for cellular automata-based algorithms, such as those used in forest fire spread simulation.



As a result of the distortion of distances due to taxigeometry, the first and more evident effect is that the familiar geometric shapes such as circles and ellipses, commonly used in forest fire simulation, have a totally different look in the taxicab and extended taxicab spaces (Figs. 8a and 8b). Together, and what is more important, the size and position of the external perimeter (i.e. fire perimeter of a propagation under uniform conditions at a certain time interval) differs greatly from what is obtained in the Euclidean space, and mostly in the angle segments multiple of  $90^\circ$  in the taxicab and of  $45^\circ$  in the extended taxicab as demonstrated above.

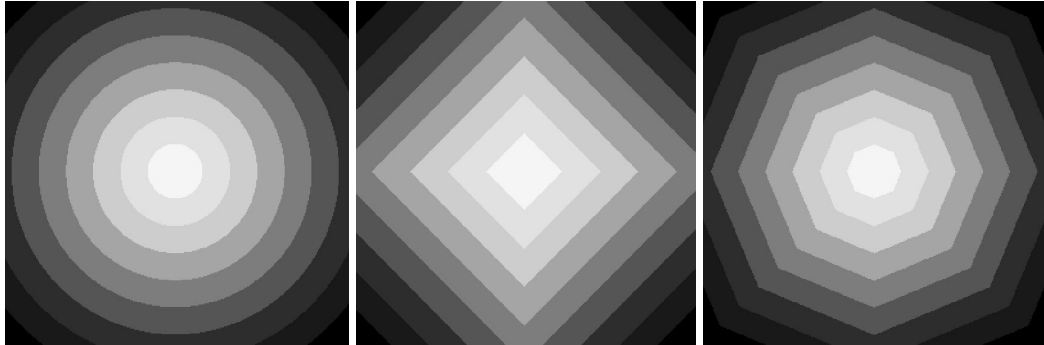


*Fig. 8a. Representation of circular isolines in the Euclidean (left), taxicab (centre) and extended taxicab (right) spaces. Although the extended taxicab solution gives octagonal shapes, which are closer to the original circular shape, still a noticeable difference is observed.*

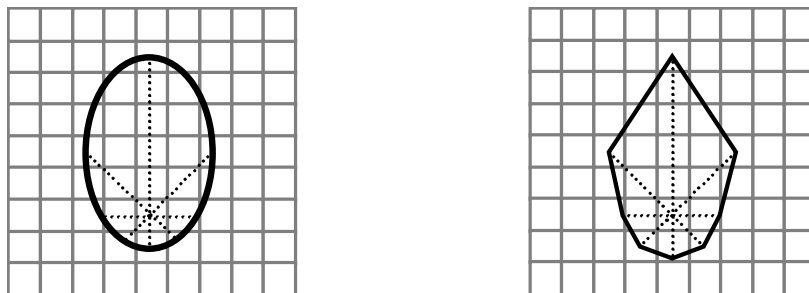


*Fig. 8b. The expected elliptical shape resulting from the spread law under uniform conditions in the Euclidean space (left) is in fact computed as a kite-like contour in the extended taxicab space of a grid map (right).*

## 5. Adopted solutions to avoid taxicab effect

To solve the identified problem of taxicab distances is not easy without entering in complex solutions. The first approach was to identify the areas in a given region that had fire spread conditions that could be assimilated as uniform, that means, the change in these conditions from reference point  $R$  and the analysed point  $B$  (see Fig. 1) fell above a set of thresholds:

- There exists different fuel model in the analysed cell  $B$  than the reference cell  $R$ .
- The slope difference between the analysed cell  $B$  and the reference cell  $R$  is greater than 10, when the slope is expressed in percentage.

- The aspect difference between the analysed cell  $B$  and the reference cell  $R$  is greater than  $15^\circ$ , when aspects are expressed in degrees.
- The wind speed difference between the analysed cell  $B$  and the reference cell  $R$  is greater than 0.5, when the wind speed is expressed in Km/h.
- The wind direction difference between the analysed cell  $B$  and the reference cell  $R$  is greater than  $15^\circ$ , when direction is expressed in degrees.

### 5.1 Propagation under uniform conditions

Using the concepts explained above, in order to avoid extended taxicab effect in the CARDIN system (Caballero; Martínez-Millán, 1990), it was proposed firstly to calculate the fire access time of a point  $B$  from a point  $R$  using directly the Euclidean distances  $RB$ , in the case that the spread conditions (slope, aspect, wind direction, wind speed) had no significant changes when compared with the reference cell  $R$ , according to the given criteria. Besides, and due to its simplicity, this immediate solution provided shorter computation times.

### 5.2 Change in propagation conditions – Huygens principle

When a significant change occur, the current analysing point  $A$  takes the role of the new reference point  $R$ , starting a new spread law from this very point (Fig. 9). This approach is similar to considering a set of pseudo-starting points (named ‘focoids’) in the places where fire propagation conditions changes, inspired in the Huygens law of wave generation in the boundary of propagation media change.

From this moment, and for further computations, the spread engine checks if there is significant difference in propagation conditions relative to the newly assigned reference point. If so, the current analysing point becomes again a new reference point; if not, the reference point is inherited to the subsequent analysed points  $B$ .

These considerations lead to calculate the distance from the analysed point  $B$  to the reference point  $R$ , instead of the analysing point  $A$ ; in some cases (frequently) the analysing point  $A$  is the same as the reference point  $R$  (in such cases where propagation conditions change). Then, the Euclidean distance and the angle correspondent to the vector  $RB$  are considered:

$$d_{RB} = \sqrt{(X_R - X_B)^2 + (Y_R - Y_B)^2}$$

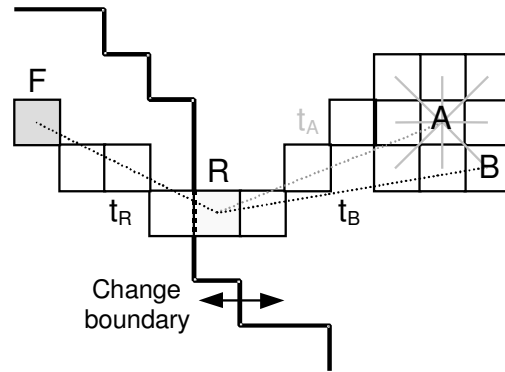


*Fig. 9. When a change in the spread conditions is found, a new starting point is generated ( $R$ ), out of which a new wave of propagation is obtained under the new conditions, much in the way it is described in the Huygens principle.*

$$\theta_{RB} = \text{ArcTan} \left( \frac{X_B - X_R}{Y_B - Y_R} \right)$$

The total access time is the sum of the time to reach the reference point  $R$  (that is  $t_R$ ) plus the time to travel from reference point  $R$  to the analysed point  $B$ , which is calculated using the basic spread law regarding each reference point. To achieve such calculation it is required to know the spread rate in the direction  $\omega_{RB}$ , obtained through the projection of the spread law belonging to the analysing cell  $A$ .

### 5.3 Continuous change in spread conditions

Nevertheless, in the real world things are never so uniform, so it seems obvious that changes will happen for every cell. With the previous presented solution taxicab effect is almost avoided, but when continuous changes happen (i.e. from cell to cell) a new correction must be applied.

In this sense, a recent new improvement to the algorithm has been implemented in the FSE application. For this, two partial distances  $D_1$  and  $D_2$  are considered (Fig. 10) for the two existing propagation conditions  $V_1$  and  $V_2$  in the vicinity of a border; in this sense, the distance from reference point to the analysing point  $AB$  is projected ( $AC$ ) onto the axis  $AB'$  connecting the reference point and the analysed point, and second, the distance from the analysing point to the analysed point  $BB'$  is projected ( $CB'$ ) in the same mentioned axis  $AB'$ .

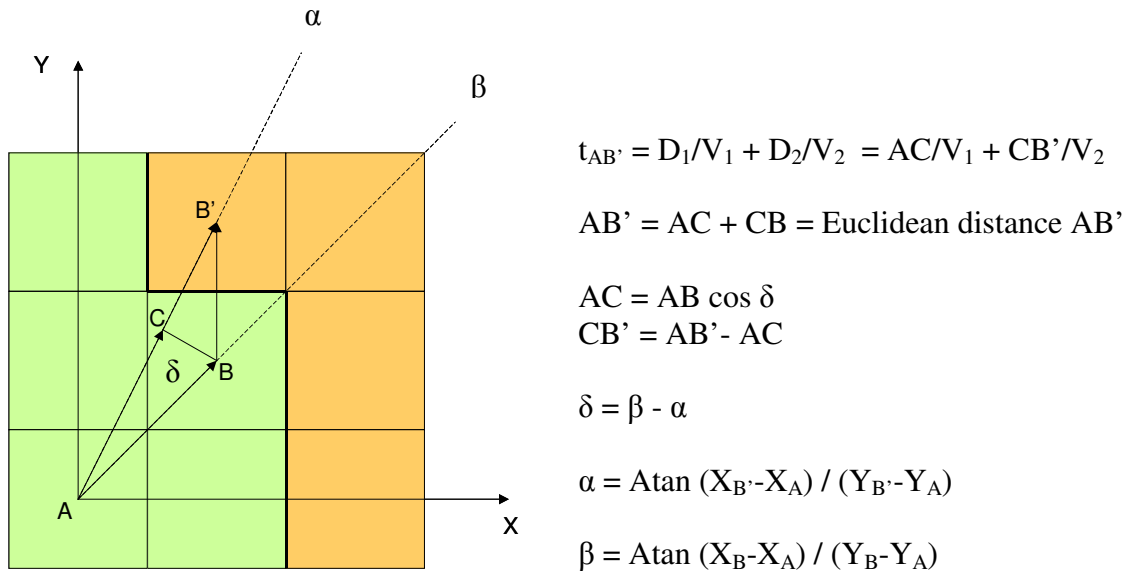


**Fig. 10.** Partial distances considered in the computation of fire access time in the case of spread condition change.

The first resulting distance  $D_1$  is used in the calculation of access time with the first spread conditions  $V_1$  (green), while the second one with the second law  $V_2$  (orange). This prevents using taxicab distances hence increasing simulation time. Instead a sum of Euclidean distances in the same projection axis is used.

## 6. A second problem: the ‘knife’ effect

Although not directly associated with taxicab geometry, but present in the computation of basic spread laws under uniform conditions in a grid map, and due to this fact, a new problem induced by this rigid geometry is found. This problem arises when the elliptical shape associated to a spread propagation is too narrow (i.e. narrower than the cell resolution) the cells placed in or near the axis of maximum spread *XDIR* are consequently associated to lower isochrones (fire access time) than those which fall apart of such axis.

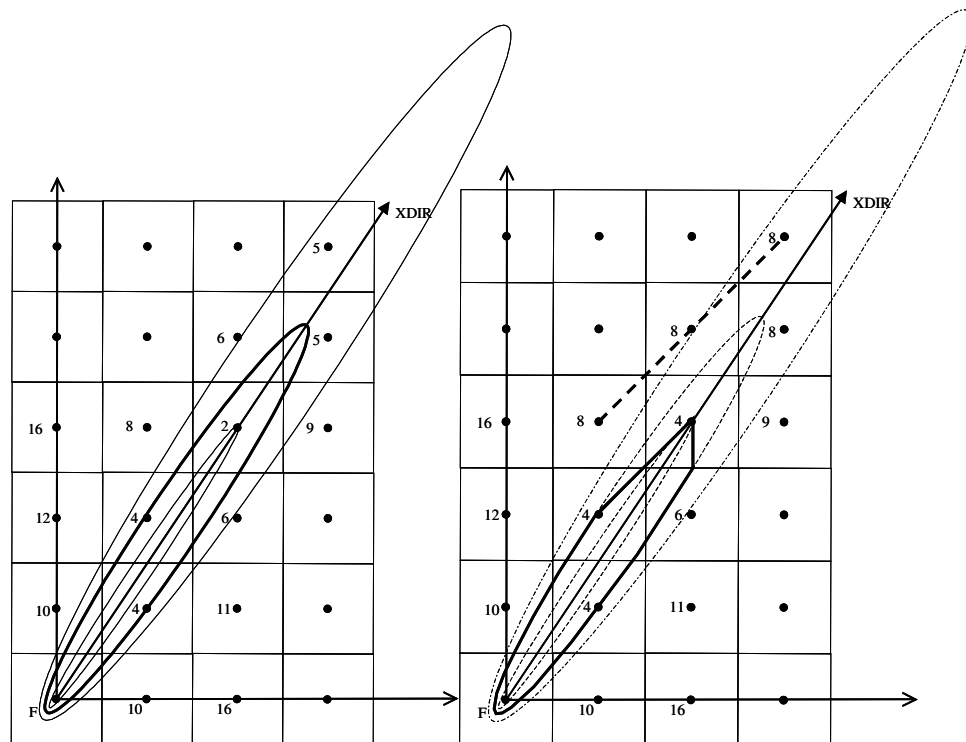
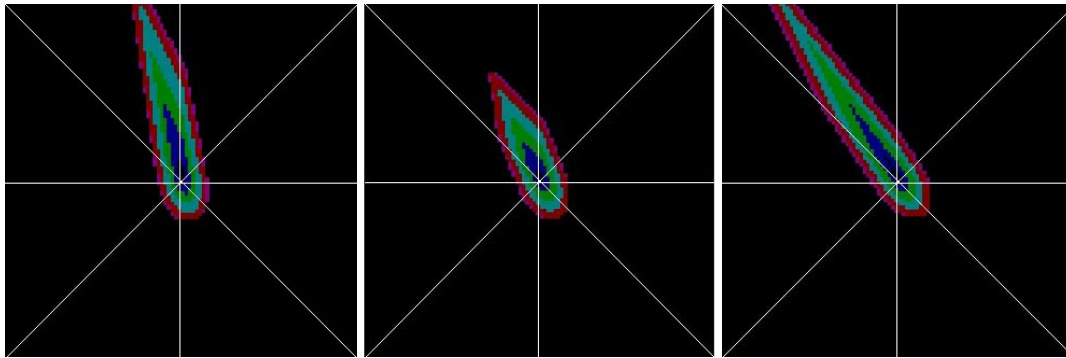


Fig. 11. The ‘knife’ effect. An example in which the fire access time to each cell is expressed in minutes, from starting point *F*. Due to this effect, the original elliptical shape (left) is distorted into a knife-like shape (right) that underestimates fire propagation

In this case, and due to the order followed in the cellular automata algorithm, the first cells analysed (those surrounding the starting point *F*) that fall apart of the axis are associated to higher time values to those cells analysed afterwards. Under such computing paradox (access time of cells analysed afterwards is lower than the analysis time, as escaping through a narrow “tunnel” in the direction of maximum spread) the algorithm assigns the current analysis time, thus consequently giving an error that is carried on in the following steps. This leads into shapes of fire spreads remembering the edge of a knife.

It is interesting to observe that the resulting shortening of the basic fire spread law in the direction of maximum spread is not constant and that, curiously, follows a pattern that is consistent with the distortion degree of distances in the extended taxicab geometry

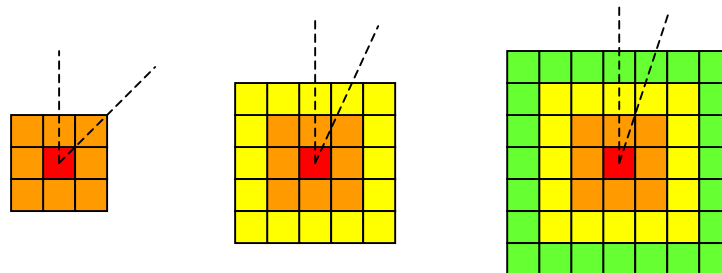
(Fig. 5). This observation has been checked in different simulations (Fig. 12), but no formal demonstration has been given yet.



**Fig. 12.** Some examples of fire spread simulations showing the 'knife' effect. Observe that the shortening of the spread law is not equal in all angles, and that it seems to follow the same pattern of distortion as that found in the distance distortion in the extended taxicab space.

## 7. Adopted solutions to avoid the 'knife' effect

To avoid this problem, a second and a third ring of cells analysed in each fire simulation iteration have been implemented in some models (i.e. FIRESTATION), but the problem persists, although is restricted to  $XDIR$  angles much closer to multiples of 45 degrees. Besides, the computation time increases noticeably.



Another solution, much more robust and implemented in this model, proposes a retro-analysis of such cells with access time lower than the analysis time and to replace the time with the actual calculated one, thus avoiding to carry on the error in the subsequent analysed cells. This approach requires that the application keeps trace of the analysed points  $B$  that give fire access time  $t_b$  which is lower than the current simulation time  $t_{sim}$ . In this case, the application compares the time  $t_b$  with the minimum one stored, if it is less then updates the minimum, remembering the  $b_x$  and  $b_y$  co-ordinates of such point:

```

if  $t_b < t_{sim}$  and  $t_b > 0$  then
    if  $t_b < \text{mint}$  and  $I(b_x, b_y) = 0$  then
         $\text{mint} = t_b$ 
         $\text{minx} = b_x$ 
         $\text{miny} = b_y$ 
    end if
end if

```

With this information stored, the application can use it for the next iteration. For this, the algorithm checks if the stored minimum time  $\text{mint}$  is less than the simulation time  $t_{\text{sim}}$ . If so, the application moves the analysis pointer to the position of the point to which this minimum time corresponds. Then the analysis continues from this point on, re-calculating this and the subsequent points taking into account the latest point analysed:

```
if  $\text{mint} < t_{\text{sim}}$  and  $\text{mint} > 0$  then
     $\text{ptr} = I(\text{minx}, \text{miny})$ 
else
     $\text{ptr} = \text{ptr} + 1$ 
end if
 $t_{\text{sim}} = t(\text{ptr})$ 
 $\text{mint} = t_{\text{sim}}$ 
```

This retro-analysis is effective, but implies to re-calculate points that have been analysed in previous iterations, hence increasing the computation time. The tests carried out with this solution, however, demonstrate its efficiency.

## 8. Current implementation of the proposed solutions

The FSE application fire spread model has been developed by the author using Real Basic® and implemented in several applications at national level in the operational plane. One of this is the SYGYM2 platform, a service provided by the private firm Meteorologica Ltd. in Spain. This service is an integrated, on-line set of GIS functionalities aimed at the prediction and of meteorological conditions and their specific application to the calculation of fire risk indexes and intrinsic values of forest fires. As a complementary application, a weblet has been developed to interact and operate the simulation system. This application has been implemented and used in Spain at regional scale during 2004 and 2005 forest fire campaigns.

Besides, the developed code is currently being currently implemented in a GRID collaborative network for risk assessment in multi-risk scenarios under the auspices of the MEDIGRID project. Implementation of the application has showed to be relatively smooth thanks to the nature of the application (stand-alone) and the data format used (ASCII GRASS) which is universal. This application will be tested in the GRID network in the 2006 fire campaign in the Mediterranean countries participating in the project.

The application has been also been implemented in a combined procedure of multi-risk analysis of river catchment, for risk prevention and natural resources management processes by TECNOMA in a region of Catalonia. This has been presented as multi-risk scenario and assessment system in the ORCHESTRA project.

## **9. Conclusions**

Digital raster maps of square cells are a good solution for the implementation of analysis algorithms for geographical values distributing continuously in the space. However, this solution entails some particularities, especially in the computation of distances, which have to be taken in consideration. The programming of cellular automata for fire spread simulation using raster maps must take in consideration that distances in the underlying geometry are not equal to the Euclidean one, except for a minimum subset of points, the so-called no-distortion axes.

The extended taxicab geometry, a modified definition of the taxicab geometry, explains and demonstrates that there is significant differences between the Euclidean and the taxicab distances. The so-called distortion map is a very useful and intuitive representation of the type and extension of such differences that programmers of such algorithms must have in mind when offering their solutions.

Together with taxicab distances, another problem associated to the rigid geometry of grid-based maps is identified, specifically when basic fire spread law is too narrow in comparison with the cell size.

As well as these, another problems can arise by the mere fact of using a solution space (square-grid maps) which constraints the real world into a rigid, pre-set geometry. Further study should be carried out to identify and describe such problems and propose new solutions.

## **10. Acknowledgements**

This paper is the result of a one-year research activity carried out mainly under the framework of EUFIRELAB project funded by the European Commission. The partial results and main reasoning lines have been presented to a number of researchers and specialists on the subject that have helped noticeably in driving the activities towards sound and interesting results.

May I acknowledge and thank here for the help and comments of Prof. Domingos Viegas, Antonio Gameiro and Miguel Cruz from ADAI, Angelos Sphiris and Vaso Varela from ALGOSYSTEMS, Mark Finney from USDA-FS, Gavriil Xanthopoulos from NAGREF and finally Gwynford Richards from the Brandon University in Canada for the publications.

## **11. References**

Caballero, D., Viegas, D.X., Xanthopoulos, G., 2001. E-FIS: an electronic on-line decision support system for forest fires. In proc. of the International Workshop on Improving Dispatching for Forest Fire Control. Mediterranean Agronomic Institute of Chania, Crete, Greece. December 6-8

Caballero, D., Xanthopoulos, G., Kallidromitou, D., Lyrintzis, G., Bonazountas, M., Papachristou, P., Pacios, O., 1999. FOMFIS: Forest Fire Management and Fire Prevention System. In proc. of DELFI Intl. Symp. Forest Fires Needs and Innovations. Pp. 93-98. Athens, Greece, 18-19 November.

Caballero, D., Martinez-Millán, F.J., Martos, J., Vignote, S., 1994. CARDIN 3.0, A Model for Forest Fire Spread and Fire Fighting Simulation. Vol.1: p.501. In proc. of 2<sup>nd</sup> Intl. Conf. on forest Fire Research. Coimbra, Portugal.

Krause, E. F., 1987. Taxicab Geometry: An Adventure in Non-Euclidean Geometry. Dover Publications, February.

Martínez-Millán, F.J. Martos, J. Vignote, S. Caballero, D. (1991). CARDIN, Un Sistema para la Simulación de la Propagación de Incendios Forestales. MAPA-INIA. Investigación Agraria Serie Recursos Naturales, Vol. 0 December